Stem Cell Reports
Article

ISSCR

OPEN ACCESS

Rapid and Efficient Conversion of Human Fibroblasts into Functional Neurons by Small Molecules

Yaming Yang,[1,3,4] Ruiguo Chen,[2,3,4] Xianming Wu,[1] Yannan Zhao,[1] Yongheng Fan,[1,3] Zhifeng Xiao,[1] Jin Han,[1] Le Sun,[2] Xiaoqun Wang,[2] and Jianwu Dai[1,*]

[1]State Key Laboratory of Molecular Developmental Biology, Institute of Genetics and Developmental Biology, Chinese Academy of Sciences, Beijing 100101, China
[2]Institute of Biophysics, Chinese Academy of Sciences, Beijing 100101, China
[3]University of Chinese Academy of Sciences, Beijing 100049, China
[4]Co-first author
*Correspondence: jwdai@genetics.ac.cn
https://doi.org/10.1016/j.stemcr.2019.09.007

SUMMARY

Recent studies have demonstrated that human astrocytes and fibroblasts can be directly converted into functional neurons by small molecules. However, fibroblasts, as a potentially better cell resource for transplantation, are not as easy to reprogram as astrocytes regarding their fate to neurons, and chemically induced neurons (iNs) with low efficiency from fibroblasts resulted in limited application for the treatment of neurological disorders, including depression. Here, we report that human fibroblasts can be efficiently and directly reprogrammed into glutamatergic neuron-like cells by serially exposing cells to a combination of small molecules. These iNs displayed neuronal transcriptional networks, and also exhibited mature firing patterns and formed functional synapses. Importantly, iNs could integrate into local circuits after transplantation into postnatal mouse brain. Our study provides a rapid and efficient transgene-free approach for chemically generating neuron-like cells from human fibroblasts. Furthermore, our approach offers strategies for disease modeling and drug discovery in central nervous system disorders.

INTRODUCTION

Direct lineage conversion transforms fully differentiated cell types by simultaneous introduction of transcription factors, and offers a promising alternative cell-based therapy for numerous major diseases. Moreover, the established technology of induced pluripotent stem cells (iPSCs) can be used to help solve the challenging problem of an unavailable and limited cell supply for cell therapy (Takahashi and Yamanaka, 2006). Even although iPSC technology is relatively easier to manipulate and provides more opportunities for generating renewable sources of multiple functional cell types, there are still significant barriers such as time-consuming induction, tumorigenesis, and indeterminate differentiation (Bellin et al., 2012). Therefore, identifying faster, safer, and more efficient strategies for generating terminally mature cells is of utmost importance for potential clinical applications, and especially cell therapies for neurological disorders.

Based on the framework of iPSC technology, and by similarly introducing cell-type-specific transcription factors, several groups have succeeded in inducing fibroblasts to functional neurons without occurrence of a dedifferentiated intermediate state or involvement of cell division (Pang et al., 2011; Vierbuchen et al., 2010). Rapid and straightforward conversion for generation of distinct neuronal subtypes such as dopaminergic neurons (Caiazzo et al., 2011), γ-aminobutyric acid (GABA)-ergic neurons (Colasante et al., 2015), and motor neurons (Son et al., 2011) makes the approach particularly convenient for cell replacement and drug discovery *in vitro*. However, inefficient neuronal conversion is a major limitation for regenerative medicine, especially when starting from human somatic cells.

Several studies have shown that chemical compounds can facilitate the developmental process and increase reprogramming efficiency to neurons by regulating specific involved signaling pathways (Chambers et al., 2012; Liu et al., 2013; Zhang et al., 2012). Although the efficiency is higher in human fetal or postnatal fibroblasts with the assistance of small molecules, adult fibroblasts are still refractory to transforming their identities under the same conditions (Ladewig et al., 2012; Liu et al., 2013). Recently, several groups have shown that small molecules can convert human astrocytes or fibroblasts into functional neurons, with a yield of up to 85% neuron generation from fetal and adult astrocytes (Gao et al., 2017; Zhang et al., 2015), which is lower from human fibroblasts, with an efficiency of no more than 15% (Hu et al., 2015). However, as resources for cell therapies, fibroblasts are better starting cells for neuronal reprogramming because of easier access for acquisition and better patient tolerance than astrocytes. Consequently, low reprogramming efficiency of human fibroblasts to neurons must be increased for broader application in neurological diseases.

Here, we screened a different set of small molecules that can efficiently convert human fibroblasts into neuron-like cells without overexpression of transcription factors. The

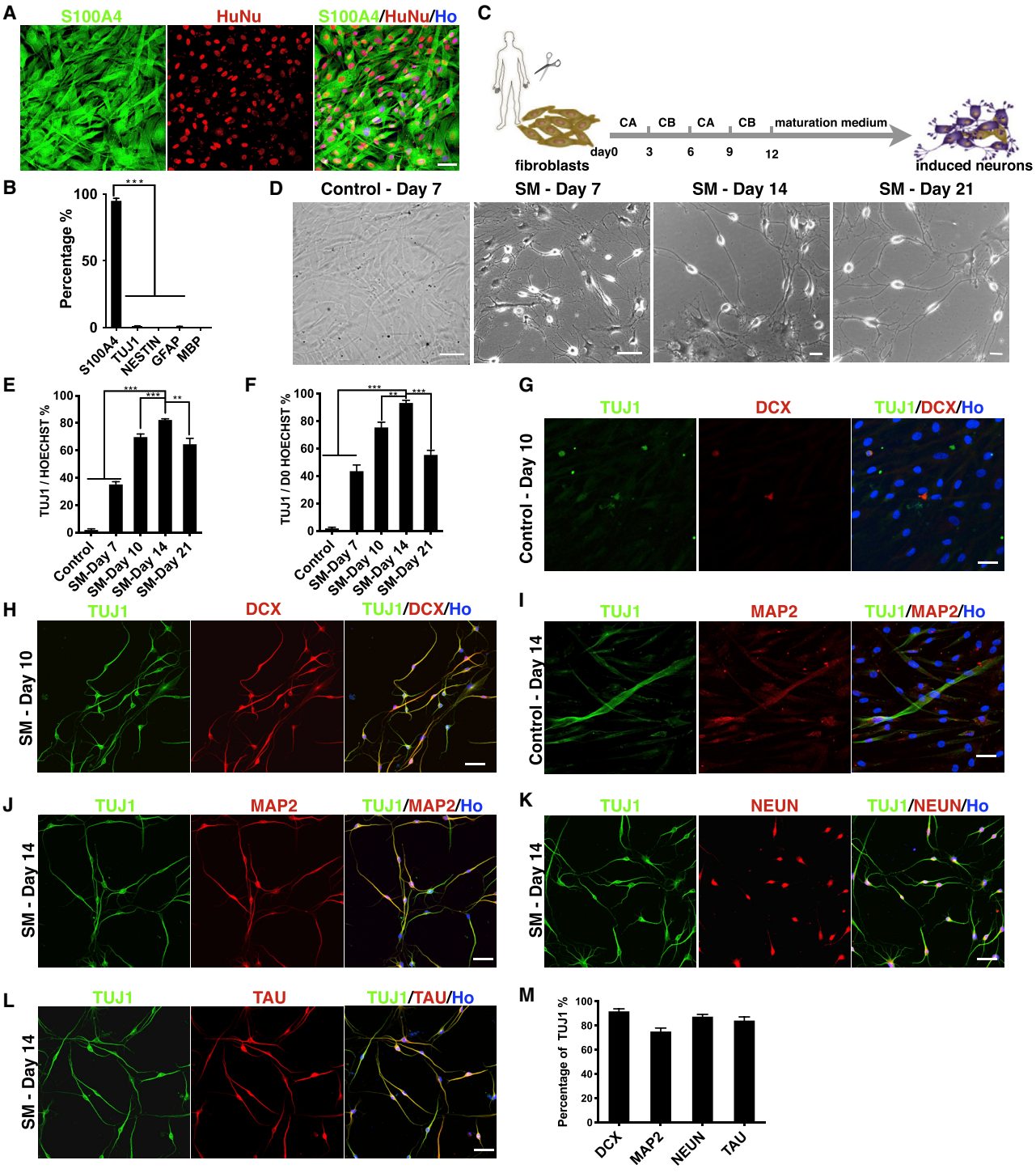

Figure 1. Small Molecules Can Efficiently Reprogram Fibroblasts to Neurons

(A and B) Identification of human newborn foreskin fibroblasts (HNFFs). (A) Immunofluorescence staining of FSP1 (green) and HuNu (red) of HNFFs. (B) Quantitative immunostaining analysis of human fibroblasts and neural lineage cells. ***$p \leq 0.001$.

(C) Schedule of experiments for reprogramming human fibroblasts to neurons using small molecules (SM).

(legend continued on next page)

rapid and efficient transgene-free approach to neuronal cell induction offers an alternative choice for disease modeling and regenerative medicine.

RESULTS

Identification of Small Molecules that Efficiently Convert Human Fibroblasts into Neurons

To efficiently convert human fibroblasts into neurons using only small molecules, we first chose a younger cell line, human newborn foreskin fibroblasts (HNFFs), which were predicted to have a higher reprogramming efficiency than older cell lines (Ladewig et al., 2012; Liu et al., 2013; Pfisterer et al., 2016). To avoid contamination of neural lineage cells in the cultured HNFFs, we examined the initial cells by immunofluorescence analysis. Appropriately, no positive signal was detected for the neural progenitor cells (NPCs) marker NESTIN, astrocytic marker glial fibrillary acidic protein, neuron marker, neuron-specific class III β-tubulin (TUJ1), or the oligodendrocytic marker, myelin basic protein (Figures S1A–S1H). To further exclude the presence of NPCs and neurons, we cultured HNFFs in neuronal induction medium for 2 weeks and did not observe any increase in genes that are highly expressed in neural lineages, as shown by real-time qRT-PCR analysis (Figure S1I). Furthermore, immunostaining showed that approximately 97% of cultured HNFFs were doubly immunopositive for the fibroblast-specific marker, fibroblast-specific protein 1 (FSP1) and the human cell-specific marker, human nuclear protein (HuNu) (Figures 1A and 1B). Altogether, these results cooperatively show no detectable contaminations of neural lineage cells in the cultured HNFFs, and confirm the purity of the preliminary cell type for the subsequent experiments.

To determine whether small molecules can rapidly and efficiently reprogram HNFFs to neurons, our initial screening identified compounds that predominantly target epigenetic modifications, metabolic activities, and signaling pathways involved in neuronal fate patterning. Based on the small molecules identified in the neural fate modulating process that differentiated from PSCs or transdifferentiated from somatic cells in previous studies (Hu et al., 2015; Ladewig et al., 2012; Liu et al., 2013; Zhang et al., 2015, 2016), we first used CHIR99021, LDN193189, SB431542, RG108, and dorsomorphin as a basic chemical neuron-induction combination and then added further new candidate small molecules on this basis (Table S1). After initial rounds of screening, we primarily screened a combination of 16 small molecules, named 16SM, which contained CHIR99021, LDN193189, SB431542, RG108, dorsomorphin, DMH1, parnate, SU5402, forskolin, Y27632, DAPT, purmorphamine, ISX9, IBET151, SU16F, and P7C3-A20. This combination led to a neuronal morphology in approximately 40% of cultured HNFFs at day 14, as shown by positive TUJ1 immunostaining (Figures S2A and S2B). To identify the essential compounds of 16SM, we sequentially removed each compound and exposed fibroblasts to the remaining factors. Exclusion of parnate and IBET151 resulted in a dramatic increase in neuronal production, while removal of SU5402, SU16F, and DMH1 had a slightly positive effect on neuronal generation. Together, the remaining 11 small molecules (11SM) were sufficient and essential for induction of neuronal reprogramming with a yield of $TUJ1^+$ cells of up to 61% (Figure S2B).

To further improve the reprogramming efficiency, we performed another round of testing. We found that addition of a mitogen-activated protein kinase inhibitor, PD0325901 (Zhu et al., 2010), further increased the yield of neuron-like cells (Figure S2C). Although the transforming growth factor β (TGFβ) type I receptor kinase (ALK-5) inhibitor, SB431542, promoted neuronal conversion from PSCs or fibroblasts (Rodriguez-Martinez and Velasco, 2012), we substituted it with A83-01, a more potent inhibitor that suppresses signaling of ALK-4, -5, and -7 and has been shown to play an important role in cell fate transformation in recent studies (Cao et al., 2016; Zhao et al., 2015).

(D) Representative morphological changes of fibroblasts after SM exposure. Phase-contrast images of cells treated with 1% DMSO at day 7 (left); or SM at day 7 (middle left), day 14 (middle right), and day 21 (right). Scale bar of two images on left, 50 μm; scale bar of two images on right, 25 μm.

(E) Quantitative analysis of $TUJ1^+$ cells by treating fibroblasts with SM for 0, 7, 10, 14, and 21 days. $^{**}p \leq 0.01$, $^{***}p \leq 0.001$.

(F) Neuronal yield after 12SM treatment was calculated as the number of $TUJ1^+$ neurons divided by the number of initial human fibroblasts. $^{**}p \leq 0.01$, $^{***}p \leq 0.001$.

(G and H) Fibroblasts treated with 1% DMSO (G) or small molecules (H) were immunostained with DCX (red) and TUJ1 (green) at day 10. Scale bars, 50 μm.

(I) Fibroblasts cultured in control (1% DMSO) medium were immunostained with MAP2 (red) and TUJ1 (green).

(J–L) Neurons induced by SM were immunopositive for MAP2 (J), NeuN (K), and TAU (L) at day 14.

(M) Neuronal conversion efficiency was represented by percentages of $DCX^+/TUJ1^+$ (91.8% ± 1.2%), $MAP2^+/TUJ1^+$ (75.2% ± 1.7%), $NeuN^+/TUJ1^+$ (87.5% ± 1.1%), and $TAU^+/TUJ1^+$ (84.1% ± 2.4%).

All data are presented as mean ± SEM, n > 3 independent experiments. Scale bars in (G) to (L), 50 μm.

Collectively, the reprogramming efficiency was significantly boosted (up to 76% TUJ1$^+$ cells at day 14) with PD0325901 and A83-01 supplementation to the 11SM cocktail (SB431542 was excluded from 12SM) (Figure S2C).

Although 12SM treatment resulted in a higher reprogramming efficiency from HNFFs to neurons, severe cell death occurred with continuous exposure for long-term culture. To reduce cell death, we decided to divide 12SM into two groups. After several rounds of attempts, we found a combination A, which mainly inhibited the fibroblast signaling pathway and initiated neural fate transformation (Figures S2D–S2F) (CA: containing CHIR99021, LDN193189, RG108, dorsomorphin, P7C3-A20, A83-01, and ISX9). The addition of combination B maintained cell survival and enhanced reprogramming efficiency (CB: containing forskolin, Y27632, DAPT, PD0325901, A83-01, purmorphamine, and P7C3-A20). A83-01 and P7C3-A20 were the mutual compounds in both groups. After several trials, we found that by adding CA and CB in a stepwise manner, as shown in Figure 1C, conversion of iNs showed a good balance of both higher efficiency and improved survival rate. However, neither CA nor CB alone could effectively generate neuron-like cells (Figures S2D and S2G). This combination of CA and CB was used in subsequent assays after the optimization of concentrations (Table S2 and Figure S2H).

When investigating the conversion process, we found that sporadic cells of fibroblasts (HNFFs) progressively shrank at day 4 while lamellipodia gradually contracted and cell soma rounded up at day 7; control wells with no small-molecule treatment (1% dimethyl sulfoxide [DMSO]) still sustained the spindle morphology of fibroblasts (Figure 1D). Reprogramming efficiency achieved a peak at day 14 (82.1% ± 1.6% TUJ1-postive cells), as shown by bright-field imaging (Figure 1D) and TUJ1 immunostaining analysis at different time points (Figure 1E). The neuronal yield was also assessed at different time points (Figure 1F). The results also indicated that efficiency at day 21 obviously decreased, which probably resulted from toxicity of small molecules. To verify this, we detected the expression of caspase-3 at days 7, 10, 14, 21, and 30 by immunostaining, and quantitative analysis showed that the apoptosis rate of iNs induced by small molecules are gradually increased after chemical treatment (Figures S2I and S2J).

To further confirm the identity of iNs, we examined immunoreactivity of a series of identified neuronal markers expressed at different neurodevelopmental stages including doublecortin (DCX), microtubule-associated protein 2 (MAP2), NeuN, and TAU. Immunostaining analysis indicated that these markers were co-expressed with TUJ1 (Figures 1H and 1J–1L), with double-positive percentage of 91.8% ± 1.2%, 75.2% ± 1.7%, 87.5% ± 1.1%, and 84.1% ± 2.4%, respectively (Figure 1M). Nearly no DCX$^+$/TUJ1$^+$ or MAP2$^+$/TUJ1$^+$ double-positive fluorescent signals were detected in the control group (Figures 1G and 1I). Taken together, these results suggest that the screened chemically defined neuronal induction medium successfully reprogrammed human fibroblasts to neurons with a high efficiency.

Small Molecules Mainly Reprogram HNFFs to Glutamatergic Neurons

To investigate specific subtypes of iNs based on released neurotransmitters, we examined the expression of vesicular glutamate transporter 1 (VGlut1) (a glutamatergic neuronal marker), GABA (a GABAergic neuronal marker), tyrosine hydroxylase (TH) (a dopaminergic neuronal marker), and choline acetyltransferase (ChAT) (a cholinergic neuronal marker) by immunoreactivity. We found that the majority of MAP2$^+$ cells were co-expressed with VGlut1 (89.1% ± 0.9%) (Figures 2A and 2E), with ≤8% MAP2$^+$ cells immunopositive for GABA (Figures 2B and 2E). Almost no positive TH$^+$ or ChAT$^+$ immunostaining signals were detected (Figures 2C–2E). To further identify specific regional identity of iNs in the central nervous system, we examined immunoreactivity of defined markers along the anterior to posterior axis. Accordingly, we found that >90% of MAP2$^+$ cells were immunopositive for the forebrain marker, forkhead box G1 (FOXG1) (Figures 2F and 2I), while only sporadic cells were immunopositive for the posterior marker, homeobox B4 (HOXB4) (Figures 2G and 2I) and midbrain marker, engrailed homeobox1 (EN1) (Figures 2H and 2I). These data indicate that the screened chemical compounds mainly induce fibroblasts toward a forebrain excitatory neuronal fate.

To determine whether human fibroblasts across different ages can be rapidly and efficiently induced to neuron-like cells using the same 12SM cocktail, we obtained human foreskin fibroblasts from 2-year-old, 29-year-old, and 36-year-old donors (abbreviated as HFF2Y, HFF29Y, and HFF36Y, respectively). Similarly, we first confirmed the cell identity and excluded the contaminations with neural lineage cells by immunostaining analysis (data not show). After sequential exposure to the same combination of small molecules, HFF2Y, HFF29Y, and HFF36Y showed morphological changes to neuron-like cells by 7 days. Furthermore, these induced morphologically neuron-like cells were also immunopositive for the neuronal markers TUJ1 and MAP2 (Figures 2J–2L) at day 14. Reprogramming efficiency of the three cell lines also reached a peak between days 10 and 14. In brief, we found that fibroblasts from younger donors were more susceptible to chemical treatment than adult fibroblasts (Figures 2M and 2N), which is in accordance with previous conclusions (Ladewig et al., 2012; Liu et al., 2013).

To explore whether 12SM can convert human fibroblasts of different origins to neurons, we obtained human fetal

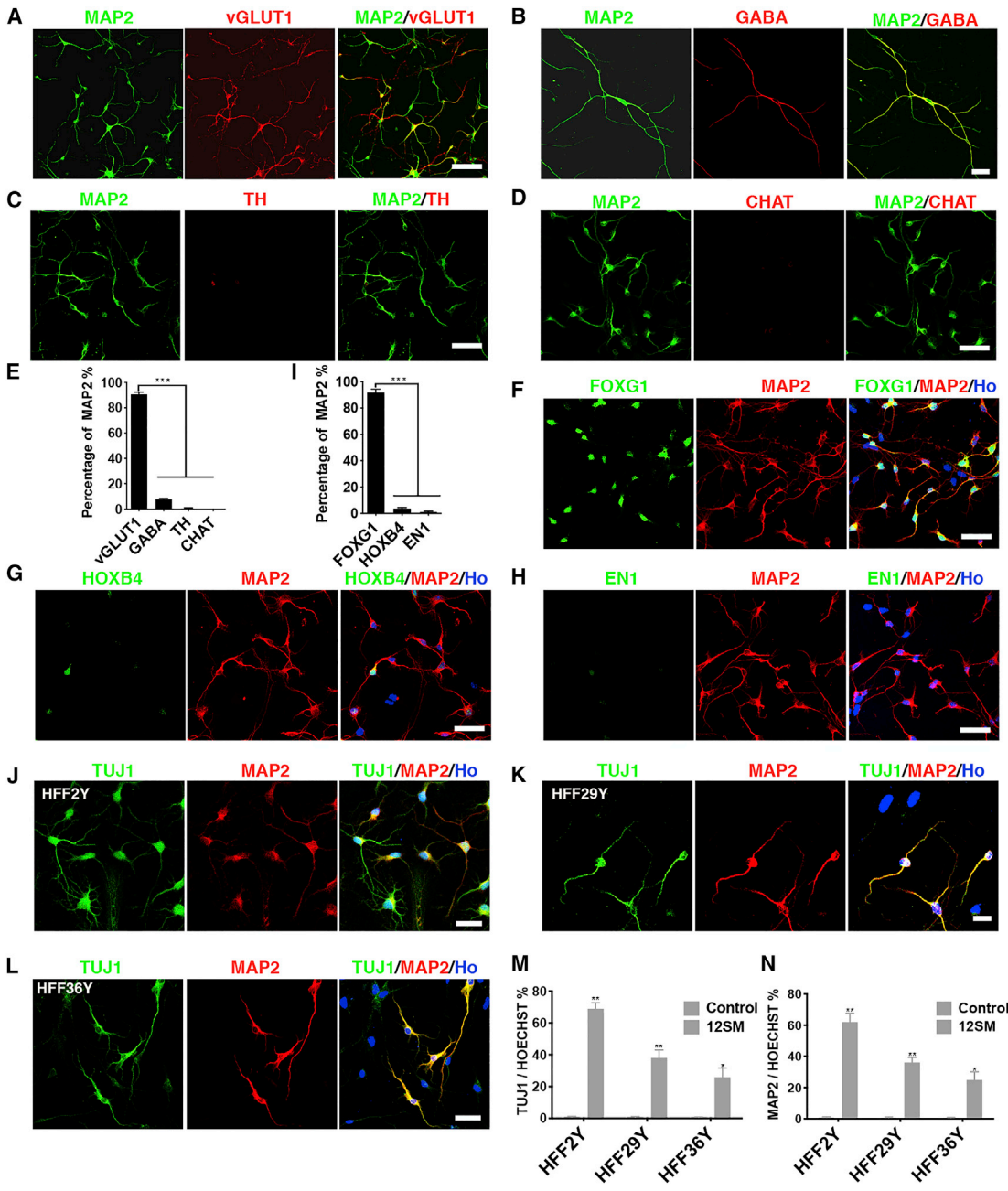

Figure 2. Characterization of Small-Molecule-Induced Neurons from Human Fibroblasts

(A–D) Immunostaining analysis of induced neurons with antibodies to MAP2 and markers of neuronal subtypes at day 14: VGlut1 (A), GABA (B), TH (C), and ChAT (D).

(E) Quantitative analysis showed no positive TH^+ or $ChAT^+$ immunostaining signal. n > 3 independent experiments; ***$p \leq 0.001$.

(F–H) Immunostaining analysis of induced neurons with antibodies to MAP2 and markers of specific regions at day 14: FOXG1 (F), HOXB4 (G), and EN1 (H).

(I) Quantitative analysis of immunostaining for region-specific markers in converted neurons. n = 4 independent batches; ***$p \leq 0.001$.

(J–L) Immunostaining analysis of iNs reprogrammed from human foreskin fibroblasts originating from 2-year-old (J), 29-year-old (K), and 36-year-old (L) donors (abbreviated HFF2Y, HFF29Y, and HFF36Y, respectively) with antibodies to TUJ1 (green) and MAP2 (red).

(M and N) Quantitative analysis of $TUJ1^+$ (68.9%, 38.0%, and 25.9%, respectively) (M) and $MAP2^+$ (61.9%, 36.0%, and 24.9%, respectively) (N) cells of HFF2Y, HFF29Y, and HFF36Y treated with 12SM. **$p \leq 0.01$.

All data are presented as mean ± SEM, n = 3 independent experiments. Scale bars, 50 μm (A–D and F–H) and 25 μm (J–L).

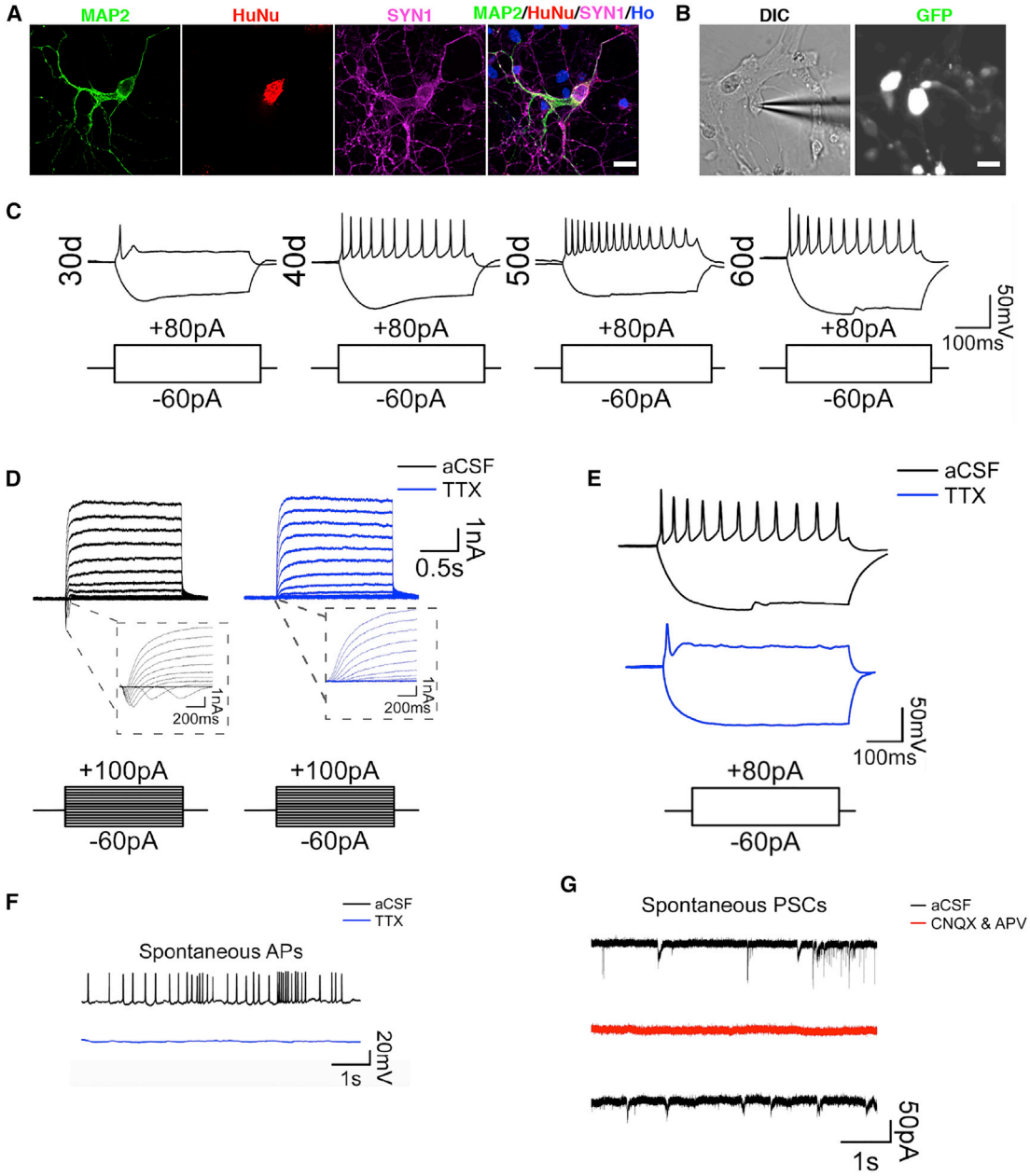

Figure 3. Induced Neurons from Fibroblasts Are Fully Mature and Electrophysiologically Functional

(A) Immunostaining of HuNu (red), synapsin I (magenta), and MAP2 (green) distinguished iNs from co-cultured astrocytes. Scale bars, 10 μm.

(B) Patch-clamp recordings were performed in iNs co-cultured with astrocytes. Bright-field image showing the pipette and cells. GFP reflects the transfected adeno-associated virus. Scale bars, 10 μm.

(C) Representative traces of voltage responses (action potentials [APs]) elicited by a series of injected currents in iNs at each development stage (from 30 days post treatment [DPT] to 60 DPT). n = 42.

(D) Representative current responses (inward and outward currents, black) evoked by a series of voltage steps (n = 29). Representative traces are shown (blue) after tetrodotoxin (TTX) treatment. Magnification of a series of inward current spikes is shown in the hashed boxes.

(E) Representative traces of APs at 40–60 DPT (black) and blockage of TTX (blue). n = 7.

(legend continued on next page)

dermal fibroblasts (HFDFs; ScienCell, catalog #2300) (Figures S3A and S3B) and exposed them to chemical-induced medium. Similar to bright-field morphological alterations of HNFFs, >75% of HFDFs gradually retracted their cytoplasm and formed globular cell bodies resembling neuron-like cells (Figure S3C). Furthermore, they expressed neuronal markers such as TUJ1, MAP2, and TAU at day 14 (Figures S3D and S3E). Analysis of related data indicated that neuronal reprogramming efficiency from HFDFs was comparable with that of HNFFs (Figure S3F). In addition, 12SM was capable of converting human adult dermal fibroblasts (ScienCell, catalog #2320) into neuron-like cells but with a lower efficiency (Figure S3G).

Human Fibroblast Transdifferentiated Neurons Are Electrophysiologically Mature

For long-term culture, we trypsinized and replated iNs on mouse primary astrocytes at 14 days post treatment (DPT) with small molecules. Immunostaining with synapsin I showed that iNs cultured on mouse astrocytes exhibited strong synaptic puncta along dendrites at 30 DPT (Figure 3A). To determine whether iNs are electrophysiologically mature in addition to the possession of morphological and immunocytochemical neuronal characteristics, we performed whole-cell patch-clamp recording. For improved targeting of iNs cultured on astrocytes, GFP-expressing adeno-associated virus was transfected to fibroblasts before exposure to small molecules (Figure 3B). We elicited action potential (AP) trains by injecting a series of currents into the soma of cultured cells (Figure 3C). In all detected iNs with APs, repetitive discharge showed that cells exhibited more mature firing patterns at 40–60 DPT (n = 33) compared with 30 DPT (n = 9) (Figure 3C). To test the existence of excitability of these cells, we next investigated the inward and outward currents evoked by a series of voltage pulses (Figure 3D). The recordings showed significant voltage-activated currents (Figure 3D, left panel) that could be blocked by tetrodotoxin (TTX) (Figure 3D, right panel). Addition of TTX also resulted in blockage of evoked APs and spontaneous APs (Figures 3E and 3F). These pharmacological results of evoked currents and APs show that these cells already have neuron-like membrane properties and activities. Furthermore, the majority of recorded cells exhibited self-driven, excitatory postsynaptic currents (ePSCs) consistent with VGlut1 expression, which could be abolished by a an AMPA/kainite receptor antagonist, CNQX, and an NMDA receptor antagonist, APV. Furthermore, the lower trace displayed the washout of CNQX, and APV recovered excitatory synaptic responses (Figure 3G). These ePSCs showed that these cells are able to connect in a mainly glutamatergic way. Altogether, these data indicated that iNs induced by the defined chemical compounds are electrophysiologically functional.

To investigate whether iNs derived from adult fibroblasts are electrophysiologically mature, we performed whole-cell patch-clamp recording around 40 days after chemical treatment. INs induced from HFF29Y and HFF36Y evoked APs by step-depolarizing the membrane in the current-clamp mode (Figures S4A–S4D). However, the ratio of iNs eliciting APs was much higher in younger iNs (42 of 63 HNFF-iNs) than that in the older iNs (5 of 13 HFF29Y-iNs and 4 of 11 HFF36Y-iNs).

RNA-Sequencing Analysis of Small-Molecule-Induced Fate Changes from Fibroblasts to Neurons

Although it turned out that 12SM was able to induce the neuronal morphological changes and stimulate expression of pan-neuronal markers, the detailed dynamic alterations were still not fully known. To address this, we performed comparative transcriptome analyses of primary neurons (PNs) derived from human embryonic brains (ScienCell, catalog #1525), nontreated HNFFs, and 12SM-treated HNFFs at days 7 and 14. First, to evaluate the overall correlation between the different cell types, we performed principal component analysis on the genome expression profiles (Figure 4A). The first three components capturing 94.32% of the total variance in the profile demonstrated obvious changes in cellular phenotype. Meanwhile, the hierarchical clustering of differentially expressed genes indicated a gradual variation in tendency from fibroblasts to neurons (Figure 4B). On the basis of gene expression profiles, we screened 26 neuron-enriched genes and 14 fibroblast-enriched genes, and showed that these genes were dramatically upregulated and downregulated in day-14 iNs and PNs, respectively. Regulated genes were substantiated by gene ontology (GO) analysis (Figure 4C). We further screened the most significant 20 upregulated genes based on their enrichment scores and established corresponding GO terms for biological processes. Surprisingly, we found that there were 14 common GO terms in both day-14 iNs and PNs when compared with fibroblasts (Figure 4D), and most of the common GO terms were associated with neuronal fate development (Figure 4E). However, the top corresponding GO terms of differentially expressed

(F) Spontaneous APs were recorded (black) at 45 DPT. No current injection was applied. Blocking the effect of TTX is shown in the blue trace (n = 11).

(G) Excitatory postsynaptic currents (ePSCs) of iNs were recorded after 45–60 DPT (upper trace). These PSCs were blocked (middle trace) by glutamatergic specific antagonists, CNQX and APV. This blockage was rescued after washout through artificial cerebrospinal fluid (aCSF) (n = 6).

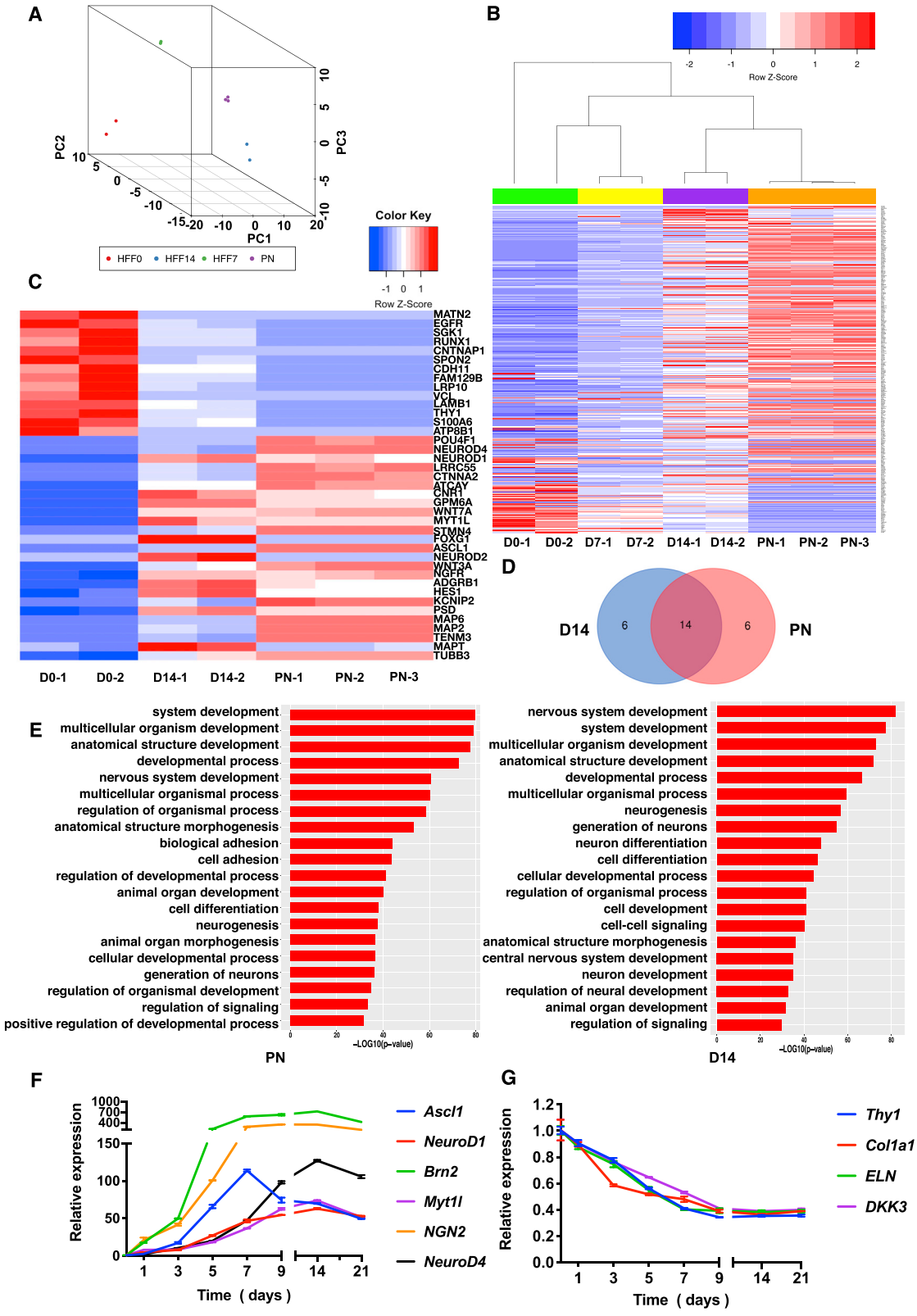

(legend on next page)

genes of day-14 iNs versus PNs indicated the synapse maturation in iNs was less than PNs to a certain degree (Figure S4E).

On the basis of gene expression profiles, 12SM gradually inhibits the development of fibroblasts and activates cell transcriptional networks resembling endogenous neurons. To further examine the early stage of the reprogramming process, we performed qRT-PCR targeting stimulation of the neural pioneer transcription factors and inhibition of fibroblast-enriched transcription factors. We found that the expression of neural-fate-determining factors was principally increased within the first 7 days, especially at days 5 and 7. Our results also show that compared with NeuroD1 and NeuroD4, neurogenin2 (Ngn2) and Ascl1 were dominant transcription factors for neuronal conversion (Figure 4F). Meanwhile, fibroblast-specific genes markedly decreased with temporal progression (Figure 4G). Taken together, these data indicate that 12SM can successfully initiate neuronal fate-determining transcription factors in conversion from fibroblasts to neurons.

Survival and Maturation of Converted Neurons *In Vivo*

To determine whether neuron-like cells induced by small molecules *in vitro* can successfully survive and mature *in vivo*, we trypsinized cultured cells at 10 DPT into single cells and collected them. Digested cells (containing reprogrammed neurons and nonreprogrammed fibroblasts) were transplanted into the cortex of neonatal immunodeficient, severe combined immunodeficiency (SCID) mice (Figure 5A). To distinguish injected human-induced neurons from host resident mouse brain neurons, we used an antibody, STEM121, which is specifically and highly expressed in the human central nervous system, in addition to the classical human-specific marker, HuNu. At 14 days post cell injection, grafted cells mainly repopulated the cortex of mouse brain, as determined by STEM121 and NeuN immunostaining (Figure 5B). At higher magnification, we observed that most STEM121$^+$ cells were also NeuN$^+$ (Figure 5C). Further immunostaining showed that the majority of transplanted cells were doubly positive for HuNu and MAP2 (Figure 5D). Two weeks later, positive synaptophysin signal was readily apparent in a portion of STEM121$^+$ cells (Figure 5E), indicating that injected iNs may integrate into local circuits. Two months after transplantation, some grafted iNs were still alive and maintained their neuronal identity, as shown by NeuN detection (Figure 5F). However, the survival rate of iNs in mouse brain gradually decreased over time (Figure 5G).

We further explored whether transplanted iNs could be electrophysiologically mature *in vivo*. To distinguish iNs from the mouse resident neurons in the brain slices, we infected human fibroblasts with EGFP before chemical treatment (Figure 5H). At 40 DPI, APs were evoked by injecting current steps in GFP-positive cells (Figure 5I), and inward sodium current responses were also elicited by a series of voltage steps (Figure 5J). Moreover, we also recorded ePSCs of GFP-positive cells (Figure 5K), which indicated that transplanted iNs could form functional synapses and integrate into local circuits.

Dissecting the Reprogramming Role of Each Compound

To evaluate the specific influences of each individual small molecule on the reprogramming processes, we implemented a series of tests by sequentially removing each compound from the 12SM mixture. Compared with the effectiveness of 12SM, absence of P7C3-A20 and ISX9 resulted in the greatest decrease of the induced neuronal number (Figures 6A–6D). Absence of purmorphamine and dorsomorphin also significantly lowered the generation of iNs (Figures 6E and 6F). Similarly, removing CHIR99021, forskolin, and LDN193189 had a negative influence on the maturity of iNs to a certain extent (Figures 6G–6I). Absence of RG108, PD0325901, and A83-01 had a slight effect on the conversion rate (Figures 6J–6L). Removal of DAPT and Y27632 had little effect on the reprogramming efficiency (Figures 6M and 6N). Quantitative analysis of NeuN (Figure 6O) also revealed that the effect of

Figure 4. Small Molecules Induced Global Transcriptional Alterations with Differentiation of Fibroblasts to Neuron-like Cells

(A) Transcriptional profiles of HNFFs, day-7 iNs, day-14 iNs, and PN are plotted along the first three principal components, which account for 68.34%, 18.53%, and 7.45%, respectively.

(B) Heatmap showing differential expression profile data of genes (fold change >2, $p < 0.05$) for samples in the following order: HNFFs, day-7 iNs, day-14 iNs, and PN. Arrays with the same name in the heatmap indicate independent biological replicates. Red indicates upregulated genes and green indicates downregulated genes.

(C) Heatmap showing differential expression of 26 neuron-enriched genes and 14 fibroblast-enriched genes in the samples. Representative genes for each group are listed (right). Red indicates upregulated genes and green indicates downregulated genes.

(D and E) Venn plot showing the most significant 20 upregulated genes based on enrichment scores (D) and established corresponding GO terms for biological processes (E) in day-14 iNs and PNs.

(F and G) Expression of determinant genes in neural development (F) and inhibition of fibroblast-specific genes (G) at days 1, 3, 5, 7, 9, 14, and 21 were validated by real-time qRT-PCR. All experiments were performed with three replicates. Data were normalized to control and presented as mean ± SEM.

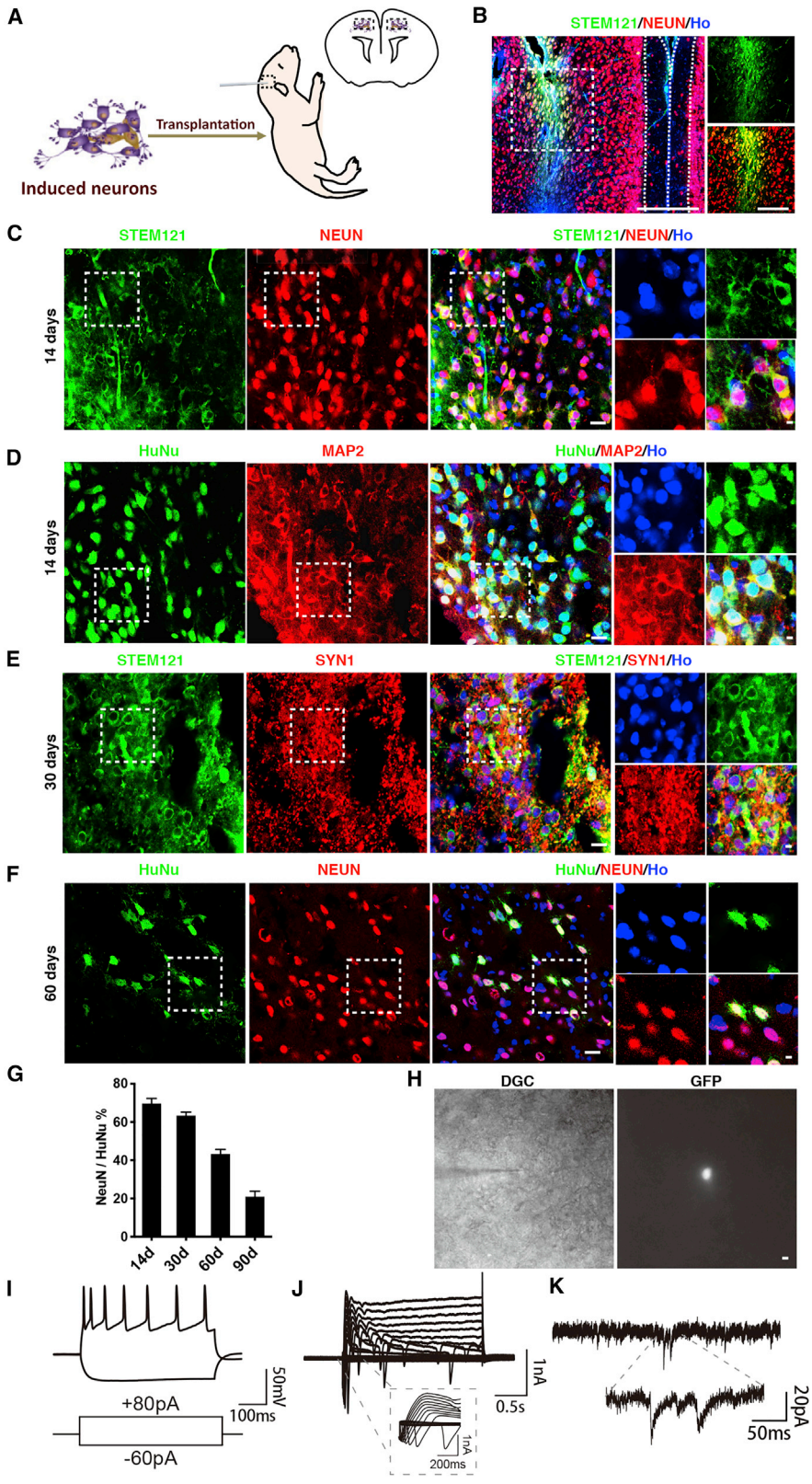

(legend on next page)

each small molecule on reprogramming efficiency was distinguished to varying degrees.

Fibroblasts Did Not Pass through a Pluripotent State to Neuronal Conversion

To determine whether the initial cell transition occurred through a pluripotent state or neural progenitor state, we examined propagation during the first 3 days and at day 5 using expression of Ki67 (Figure S5A), which is widely regarded as a proliferation marker. Immunostaining showed that exposing fibroblasts to 12SM cocktail resulted in markedly reduced proliferative ability during the first 2 days, with only 10% of cultured cells showing a positive Ki67 signal at day 2, which was barely noticeable at day 5 (Figure S5B). However, the expression of Ki67 did not show obvious changes when cells were cultured in control medium or fibroblast medium (Figures S5C and S5D). To further examine the reprogramming process at the early stages, we collected treated cells at the same time points and performed qRT-PCR primarily focused on genes highly expressed in PSCs or neural stem cells, including octamer-binding transcription factor 4 (*OCT4*), nanog homeobox (*NANOG*), sex-determining region Y-box 2 (*SOX2*), *NESTIN*, and paired box 6 (*PAX6*) (Figure S5E). We found that these enriched genes in pluripotent and neural stem cells were barely detected by qRT-PCR, and almost no positive signals were apparent by immunostaining (data not shown) in early stages after 12SM treatment. These results imply that the reprogramming process is directly induced and does not exhibit a dedifferentiated intermediate toward a highly proliferated pluripotent or neural stem cell.

The Different Reprogramming Progress of iNs Induced by VCRFSGY and 12SM

To further detail the differences of reprogramming progress between VCRFSGY (VPA, CHIR99021, RepSox, forskolin, SP600625, GO6983, and Y-27632) in the previous report (Hu et al., 2015) and 12SM, we observed the dynamic morphological responses to different treatments in early stages (Figure S6A). We found that HNFF morphologies were significantly changed after exposure to VCRFSGY at day 1, whereas cells treated with 12SM were basically consistent with these cultured in medium without small molecules. However, the morphological changes from fibroblasts to neurons in 12SM-treated groups were gradually increased and slightly higher than that in VCRFSGY-treatment groups at day 3. The reprogramming efficiency in 12SM-treated groups was still enhanced from day 3 to day 7, but in VCRFSGY-treatment groups there were no obvious neuronal morphological changes at the same time. At later stages, there were no more significant changes in both groups treated with small molecules. We found that reprogramming conditions of dynamic changes in HFF-29Y were similar to those of HNFF but with a lower efficiency (Figure S6B).

DISCUSSION

In this study, our results show that human fibroblasts can be efficiently reprogrammed to functional neuron-like cells over a period of 10 days by treatment with 12 chemical compounds in a stepwise additive manner. In addition, these iNs could survive for at least 2 months and exhibited robust electrophysiological activity when co-cultured with astrocytes. Furthermore, after transplanting the converted neurons into the mouse brain, the cells could successfully survive *in vivo* and integrate into resident circuits.

In our screening of effective small molecules for reprogramming neuronal conversion, we mainly focused on chemicals known to play important roles in the neural fate patterning, especially signaling pathways, including

Figure 5. Survival and Maturation of Converted Neurons *In Vivo*

(A) Experimental schedule for transplantation of chemical compound-converted human neurons into postnatal mouse cortex.
(B) Transplanted human iNs were identified in the cortex by immunostaining with STEM121 (green) and NeuN (red) at 14 days post injection (14 DPI). n = 4 mice.
(C) Positive immunostaining signals for STEM121 (green) and NeuN (red) were detected at 14 DPI.
(D) Transplanted small-molecule-converted neurons co-expressed HuNu (green) and MAP2 (red) at 14 DPI.
(E) Transplanted small-molecule-converted neurons were doubly immunopositive for STEM121 (green) and synapsin I (SYNI, red) at 30 DPI. n = 3 mice.
(F) Transplanted iNs survived more than 2 months *in vivo* and were identified by co-expression with HuNu (green) and NeuN (red). n = 3 mice.
(G) Quantitative analysis of survival rate of transplanted neurons at different times *in vivo* (n = 3 mice at each stage).
(H) The representative bright-field and GFP images of whole-cell recording from GFP-positive cells in brain slices.
(I) Action potentials were evoked by injecting current steps in GFP-positive cells (n = 10).
(J) Representative current responses (inward and outward currents) evoked by a series of voltage steps. Magnification of a series of inward current spikes is shown in the hashed boxes (n = 12).
(K) Excitatory postsynaptic currents (ePSCs) of converted neurons were recorded at days 30–40 (n = 6).
All data are presented as mean ± SEM. Scale bars, 100 μm (B), 25 μm (C–F, larger images), 10 μm (C–F, smaller images) and 10 μm (H).

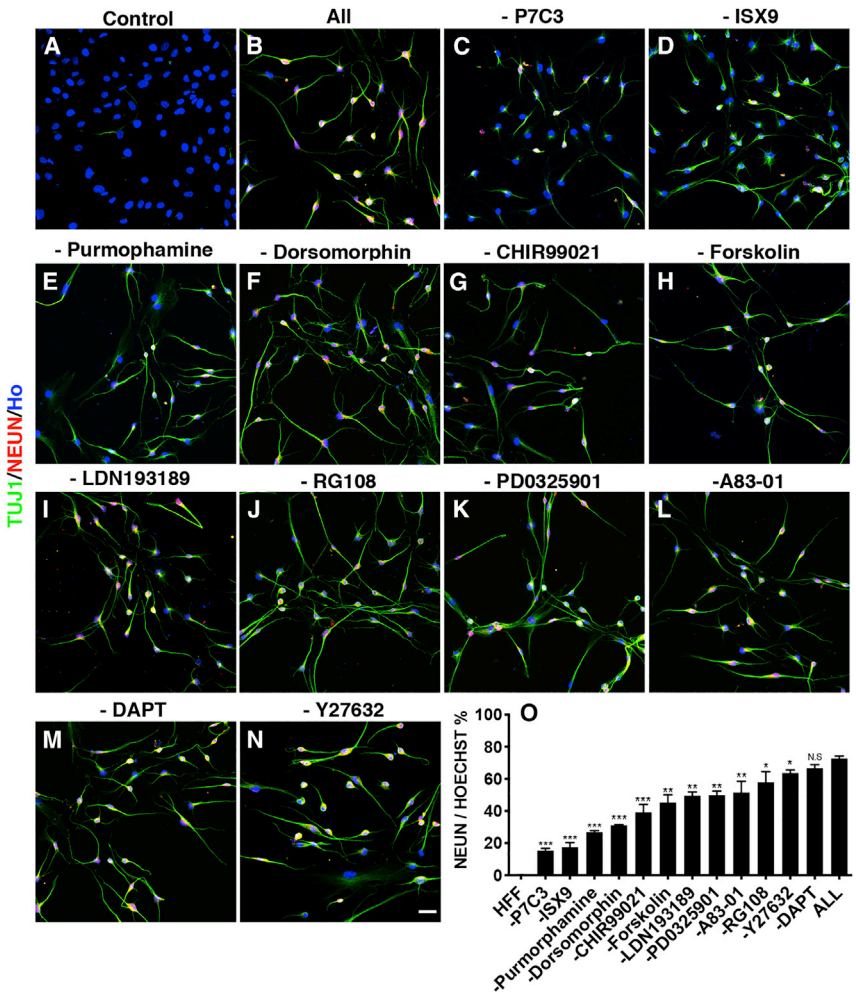

Figure 6. Assessing the Individual Role of Each Chemical Compound in the Reprogramming Process

(A) Immunostaining of TUJ1 and NeuN of HNFFs cultured in control medium for 14 days.

(B) Immunostaining of TUJ1 and NeuN of HNFFs exposed to 12SM medium for 14 days.

(C–N) Immunofluorescence staining of TUJ1 and NeuN of HNFFs by sequentially removing P7C3 (C), ISX9 (D), purmophamine (E), dorsomorphin (F), CHIR99021 (G), forskolin (H), LDN193189 (I), RG108 (J), PD0325901 (K), A83-01 (L), DAPT (M), and Y27632 (N) from the 12SM mixture. Scale bar in (N), 50 μm (applies to all images).

(O) Quantitative analysis of $NeuN^+$ cells induced by small molecules. Data are presented as mean ± SEM, n = 3 independent experiments; *p < 0.05, **p < 0.01, ***p < 0.001.

TGFβ, GSK3β, WNT, sonic hedgehog, retinoic acid (RA), and bone morphogenetic protein. Epigenetic reprogramming is another point to consider in fate transformation. Consequently, we screened several small molecules modulating DNA methylation and histone methylation and identified RG108 (a DNA methyltransferases inhibitor) and parnate (a lysine-specific demethylase 1 inhibitor) as candidates for 16SM. Surprisingly, we found that removal of parnate markedly increased the reprogramming efficiency, which is consistent with previous results in the primary screen (Cao et al., 2016). However, exclusion of RG108 decreased the number of TUJ1-positive cells. Compared with parnate, RG108 is a non-nucleoside DNA methyltransferase that is less damaging to DNA and less toxic to cells. RG108 also shows lower demethylation and gene re-expression activity (Fandy, 2009). Even though parnate has higher activity, its addition may negatively affect the activity of the remaining small molecules in the cocktail, and it is involved in other signaling pathways, ultimately resulting in inefficient reprogramming.

In these removal experiments, our results show that P7C3-A20 and ISX9 are the two most significant components in the neuronal reprogramming. Compared with inefficient reprogramming induced by VCRFSGY, our removal experiments suggest that addition of P7C3-A20, ISX9, and purmorphamine may play significant roles in efficient fate transformation from fibroblasts to neurons. P7C3 is a nicotinamide phosphoribosyl transferase (NAMPT) that has a profoundly neuroprotective impact on neurological diseases with cognitive decline, including Parkinson's disease (De Jesus-Cortes et al., 2012), amyotrophic lateral sclerosis (Tesla et al., 2012), and traumatic brain injury (Loris et al., 2017). P7C3-A20 is a derivative of P7C3 and a highly effective neuroprotective compound that promotes neurogenesis and inhibits cell death of mature neurons (MacMillan et al., 2011; Pieper et al., 2014). During the postnatal neurogenesis process, nicotinamide adenine dinucleotide (NAD) and NAMPT play important roles (Wang et al., 2016) in neural generation and neuronal survival. It has been demonstrated that P7C3-A20 binds to

NAMPT, which is a rate-limiting enzyme in the NAD biosynthetic process (Wang et al., 2014). In this context, P7C3-A20 may stimulate NAMPT-relevant pathways to exert neurogenesis and neuroprotection in fate transformation from fibroblasts to neurons. ISX9 is also a synthetic chemical compound with an effective role in neuronal generation (Schneider et al., 2008). Moreover, previous reports have confirmed that Isx9 plays an important role in the initiation of neuronal fate from mouse embryonic fibroblasts (Li et al., 2015) and human adult astrocytes (Gao et al., 2017). Although the specific mechanisms for effectiveness of ISX9 in the chemical compounds-driven reprogramming are unclear, its functional role in increasing neurogenesis and memory in the adult hippocampus *in vivo* suggests the participation of the myocyte-enhancer family of proteins (MEF2) (Petrik et al., 2012). MEF2 family members are identified as important regulators in modulating neurite growth of TUJ1-expressing neurons *in vitro* and embryonic neural stem cell differentiation *in vivo* in the developing nervous system (Lam and Chawla, 2007). In combination with the positive impacts of ISX9 on the other cell systems (Dioum et al., 2011; Zhang et al., 2011), additional studies are necessary to clarify the specific mechanisms of small-molecule-induced reprogramming from fibroblasts to neurons.

Although many reports have demonstrated that small molecules can convert one type of terminally differentiated somatic cell to another fully differentiated cell type, there are still various major hurdles ahead that must be overcome. One of the most prominent problems is how small molecules can be used to coax the initial cells toward a unique cell line for reprogramming. The beginning of successful small-molecule-driven cell reprogramming effectively inhibits signaling pathways enriched in the initial cells. As a result, suppressing the TGFβ signaling pathway (e.g., with A83-01 or RepSox) and stimulating the WNT signaling pathway (e.g., with CHIR99021) in mouse or human fibroblasts are common factors considered in reprogramming (Cao et al., 2016; Fu et al., 2015; Hu et al., 2015; Li et al., 2015). Besides, the successful conversion involves synchronous addition of particular developmental growth factors (such as brain-derived neurotrophic factor and neurotrophin-3 for neurodevelopment, and vascular endothelial growth factor for vasculogenesis), and small molecules modulating lineage-specific development-related signaling pathways. However, compared with transcription factor-induced reprogramming, which is only required for participation of fate-determining transcription factors of relevant cells, in most cases small molecules mediating cell transformation are not as specific as these latter methods. Another challenge is the difficulty of obtaining more specific types of neurons with higher purity. Based on previously published data (Hu et al., 2015; Li et al., 2015; Zhang et al., 2015) and the results of our studies, iNs in most conditions tend to be glutamatergic subtypes, and only a small proportion of cells expressing GABAergic markers are induced by small molecules. Even though we added specific neuronal development-related factors (such as RA and fibroblast growth factor 8) to 12SM in this study, it was still difficult to influence iNs subtypes without the assistance of transcription factors. This suggests that small-molecule-induced reprogramming still has various problems that urgently need to be resolved before the technology can be put into practice.

Regardless of the challenges, rapid and efficient reprogramming from human fibroblasts to neurons by small molecules offers an alternative strategy for neuronal regeneration. Meanwhile, further detailed mechanistic investigation of the reprogramming process based on chemical compounds will provide a platform for gaining insight into neurological disease modeling and drug screening.

EXPERIMENTAL PROCEDURES

Generation of Induced Neurons from Human Fibroblasts by Small Molecules

Fibroblasts were first cultured on poly-D-lysine-coated coverslips in 24-well plates with 10,000–15,000 cells/well. Cells were maintained in fibroblast medium for 24 h. Next, medium was completely replaced by neuronal induction medium (NIM) consisting of DMEM/F12:neurobasal medium (1:1) supplemented with 1% N-2, 2% B-27, 40 ng/mL brain-derived neurotrophic factor, 20 ng/mL glial cell-derived neurotrophic factor, 20 ng/mL insulin-like growth factor 1, and 1 mM GlutaMAX. NIM also contained small molecules or 1% DMSO in control groups. Fibroblasts were treated with NIM containing CA (3 μM CHIR99021, 0.25 μM LDN193189, 10 μM RG108, 1 μM dorsomorphin, 3 μM P7C3-A20, 0.5 μM A83-01, and 5 μM ISX9). Three days later, half the medium was changed to NIM containing CB (10 μM forskolin, 5 μM Y27632, 1 μM DAPT, 1 μM PD0325901, 0.5 μM A83-01, 1 μM purmorphamine, and 3 μM P7C3-A20) for another 3 days. Half the medium was again changed with NIM containing CA or CB for another round. At day 12, half the medium was changed to neuronal maturation medium (NMM): NIM supplemented with 20 ng/mL neurotrophin-3 (NT-3) and 2 μM Y27632. Half of NMM was refreshed every 2 days. Information on all small molecules used in this study are listed in Tables S1 and S2.

Electrophysiology

Whole-cell patch-clamp recordings of iNs *in vitro* or in brain slices were performed as described in detail in Supplemental Experimental Procedures and Table S3.

Cell Culture

Human foreskin fibroblasts with different ages were obtained from dissociated foreskin tissue of healthy donors provided by The 306th Hospital of The People's Liberation Army of China. Human fetal and adult dermal skin fibroblasts were purchased from

ScienCell (catalog #2300 and #2320, respectively). The details of fibroblasts used in this study are provided in Table S4. Fibroblasts were cultured in DMEM high-glucose medium (Invitrogen) consisting of 10% fetal bovine serum (Gibco), 1% nonessential amino acids (Gibco), and 1 mM GlutaMAX (Gibco). Medium was changed every 2 days. Human foreskin fibroblasts derived from donors were approved for collection and application by institutional ethical committees. The culture of human fetal neural stem cells is described in detail in Supplemental Experimental Procedures.

Immunocytochemistry

Cells were fixed with 4% paraformaldehyde, washed four times with PBS, and blocked with PBS buffer containing 5% (v/v) normal donkey serum and 0.1% Triton X-100 for 1 h at room temperature before being incubated in primary antibodies (see Table S5) overnight at 4°C. Secondary antibodies were then incubated for 40 min at room temperature and mounted in Mounting Medium with DAPI. Images were observed with a Zeiss Axio Scope A1 and captured with Zeiss LSM 710 confocal laser scanning microscope.

RNA Isolation and qRT-PCR

Total RNA was extracted using TRIzol reagent (Invitrogen, #15596-018). One microgram of total RNA was reverse transcribed to cDNA by a Hifair III First Strand cDNA Synthesis kit (gDNA digester plus) (Yeasen, #11141ES10) following the instruction manual. qPCR was performed with the CFX96 T Real-Time System (Bio-Rad). The primer sequences and details are listed in Table S6.

Cell Transplantation

All studies on mice were performed in line with the animal policy of the Institute of Genetics and Developmental Biology, Chinese Academy of Sciences. Cultured chemically induced neurons were dissociated with 0.05% Trypsin-EDTA (Gibco) into single cells and centrifuged for 3 min at 800 rpm. Cell deposits were collected and resuspended at a density of $1 \times 10^5/\mu L$ in NIM. Cells were then injected into the brain of SCID mice. The specific methods are described in detail in Supplemental Experimental Procedures.

Statistical Analysis

Statistical analyses were performed by Student's t test. Quantitative data are presented as means ± SEM of at least three independent experiments. Probabilities of $p < 0.05$ were considered as significant ($^*p \leq 0.05$, $^{**}p \leq 0.01$, and $^{***}p \leq 0.001$ in figures).

ACCESSION NUMBERS

Sequencing data for the RNA sequencing reported in this study have been submitted to the NCBI Sequence Read Archive under accession number NCBI: SRP150612.

SUPPLEMENTAL INFORMATION

Supplemental Information can be found online at https://doi.org/10.1016/j.stemcr.2019.09.007.

AUTHOR CONTRIBUTIONS

Y.Y., R.C., and J.D. conceived and designed the experiments. Y.Y., R.C., and Y.F. performed the experiments. Y.Y., R.C., and X.W. analyzed the data. Y.Z., Z.X., J.H., L.S., and X.W. provided advice. Y.Y. and R.C. wrote the manuscript.

ACKNOWLEDGMENTS

This work was supported by grants from the Strategic Priority Research Program of the Chinese Academy of Sciences (XDA16020100), the Key Research Program of the Chinese Academy of Sciences (grant no. ZDRW-ZS-2016-2), and the National Key R&D Program of China (2017YFA0104700).

Received: December 5, 2018
Revised: September 17, 2019
Accepted: September 17, 2019
Published: October 17, 2019

REFERENCES

Bellin, M., Marchetto, M.C., Gage, F.H., and Mummery, C.L. (2012). Induced pluripotent stem cells: the new patient? Nat. Rev. Mol. Cell Biol. *13*, 713–726.

Caiazzo, M., Dell'Anno, M.T., Dvoretskova, E., Lazarevic, D., Taverna, S., Leo, D., Sotnikova, T.D., Menegon, A., Roncaglia, P., Colciago, G., et al. (2011). Direct generation of functional dopaminergic neurons from mouse and human fibroblasts. Nature *476*, 224–227.

Cao, N., Huang, Y., Zheng, J.S., Spencer, C.I., Zhang, Y., Fu, J.D., Nie, B.M., Xie, M., Zhang, M.L., Wang, H.X., et al. (2016). Conversion of human fibroblasts into functional cardiomyocytes by small molecules. Science *352*, 1216–1220.

Chambers, S.M., Qi, Y.C., Mica, Y., Lee, G., Zhang, X.J., Niu, L., Bilsland, J., Cao, L.S., Stevens, E., Whiting, P., et al. (2012). Combined small-molecule inhibition accelerates developmental timing and converts human pluripotent stem cells into nociceptors. Nat. Biotechnol. *30*, 715.

Colasante, G., Lignani, G., Rubio, A., Medrihan, L., Yekhlef, L., Sessa, A., Massimino, L., Giannelli, S.G., Sacchetti, S., Caiazzo, M., et al. (2015). Rapid conversion of fibroblasts into functional forebrain GABAergic interneurons by direct genetic reprogramming. Cell Stem Cell *17*, 719–734.

De Jesus-Cortes, H., Xu, P., Drawbridge, J., Estill, S.J., Huntington, P., Tran, S., Britt, J., Tesla, R., Morlock, L., Naidoo, J., et al. (2012). Neuroprotective efficacy of aminopropyl carbazoles in a mouse model of Parkinson disease. Proc. Natl. Acad. Sci. U S A *109*, 17010–17015.

Dioum, E.M., Osborne, J.K., Goetsch, S., Russell, J., Schneider, J.W., and Cobb, M.H. (2011). A small molecule differentiation inducer increases insulin production by pancreatic beta cells. Proc. Natl. Acad. Sci. U S A *108*, 20713–20718.

Fandy, T.E. (2009). Development of DNA methyltransferase inhibitors for the treatment of neoplastic diseases. Curr. Med. Chem. *16*, 2075–2085.

Fu, Y., Huang, C., Xu, X., Gu, H., Ye, Y., Jiang, C., Qiu, Z., and Xie, X. (2015). Direct reprogramming of mouse fibroblasts into cardiomyocytes with chemical cocktails. Cell Res. *25*, 1013–1024.

Gao, L., Guan, W., Wang, M., Wang, H., Yu, J., Liu, Q., Qiu, B., Yu, Y., Ping, Y., Bian, X., et al. (2017). Direct generation of human neuronal cells from adult astrocytes by small molecules. Stem Cell Reports *8*, 538–547.

Hu, W., Qiu, B., Guan, W., Wang, Q., Wang, M., Li, W., Gao, L., Shen, L., Huang, Y., Xie, G., et al. (2015). Direct conversion of normal and Alzheimer's disease human fibroblasts into neuronal cells by small molecules. Cell Stem Cell *17*, 204–212.

Ladewig, J., Mertens, J., Kesavan, J., Doerr, J., Poppe, D., Glaue, F., Herms, S., Wernet, P., Kogler, G., Muller, F.J., et al. (2012). Small molecules enable highly efficient neuronal conversion of human fibroblasts. Nat. Methods *9*, 575–578.

Lam, B.Y., and Chawla, S. (2007). MEF2D expression increases during neuronal differentiation of neural progenitor cells and correlates with neurite length. Neurosci. Lett. *427*, 153–158.

Li, X., Zuo, X., Jing, J., Ma, Y., Wang, J., Liu, D., Zhu, J., Du, X., Xiong, L., Du, Y., et al. (2015). Small-molecule-driven direct reprogramming of mouse fibroblasts into functional neurons. Cell Stem Cell *17*, 195–203.

Liu, M.L., Zang, T., Zou, Y.H., Chang, J.C., Gibson, J.R., Huber, K.M., and Zhang, C.L. (2013). Small molecules enable neurogenin 2 to efficiently convert human fibroblasts into cholinergic neurons. Nat. Commun. *4*, 2183.

Loris, Z.B., Pieper, A.A., and Dietrich, W.D. (2017). The neuroprotective compound P7C3-A20 promotes neurogenesis and improves cognitive function after ischemic stroke. Exp. Neurol. *290*, 63–73.

MacMillan, K.S., Naidoo, J., Liang, J., Melito, L., Williams, N.S., Morlock, L., Huntington, P.J., Estill, S.J., Longgood, J., Becker, G.L., et al. (2011). Development of proneurogenic, neuroprotective small molecules. J. Am. Chem. Soc. *133*, 1428–1437.

Pang, Z.P., Yang, N., Vierbuchen, T., Ostermeier, A., Fuentes, D.R., Yang, T.Q., Citri, A., Sebastiano, V., Marro, S., Sudhof, T.C., et al. (2011). Induction of human neuronal cells by defined transcription factors. Nature *476*, 220–223.

Petrik, D., Jiang, Y., Birnbaum, S.G., Powell, C.M., Kim, M.S., Hsieh, J., and Eisch, A.J. (2012). Functional and mechanistic exploration of an adult neurogenesis-promoting small molecule. FASEB J. *26*, 3148–3162.

Pfisterer, U., Ek, F., Lang, S., Soneji, S., Olsson, R., and Parmar, M. (2016). Small molecules increase direct neural conversion of human fibroblasts. Sci. Rep. *6*, 38290.

Pieper, A.A., McKnight, S.L., and Ready, J.M. (2014). P7C3 and an unbiased approach to drug discovery for neurodegenerative diseases. Chem. Soc. Rev. *43*, 6716–6726.

Rodriguez-Martinez, G., and Velasco, I. (2012). Activin and TGF-beta effects on brain development and neural stem cells. CNS Neurol. Disord. Drug Targets *11*, 844–855.

Schneider, J.W., Gao, Z., Li, S., Farooqi, M., Tang, T.S., Bezprozvanny, I., Frantz, D.E., and Hsieh, J. (2008). Small-molecule activation of neuronal cell fate. Nat. Chem. Biol. *4*, 408–410.

Son, E.Y., Ichida, J.K., Wainger, B.J., Toma, J.S., Rafuse, V.F., Woolf, C.J., and Eggan, K. (2011). Conversion of mouse and human fibroblasts into functional spinal motor neurons. Cell Stem Cell *9*, 205–218.

Takahashi, K., and Yamanaka, S. (2006). Induction of pluripotent stem cells from mouse embryonic and adult fibroblast cultures by defined factors. Cell *126*, 663–676.

Tesla, R., Wolf, H.P., Xu, P., Drawbridge, J., Estill, S.J., Huntington, P., McDaniel, L., Knobbe, W., Burket, A., Tran, S., et al. (2012). Neuroprotective efficacy of aminopropyl carbazoles in a mouse model of amyotrophic lateral sclerosis. Proc. Natl. Acad. Sci. U S A *109*, 17016–17021.

Vierbuchen, T., Ostermeier, A., Pang, Z.P., Kokubu, Y., Sudhof, T.C., and Wernig, M. (2010). Direct conversion of fibroblasts to functional neurons by defined factors. Nature *463*, 1035–1041.

Wang, G., Han, T., Nijhawan, D., Theodoropoulos, P., Naidoo, J., Yadavalli, S., Mirzaei, H., Pieper, A.A., Ready, J.M., and McKnight, S.L. (2014). P7C3 neuroprotective chemicals function by activating the rate-limiting enzyme in NAD salvage. Cell *158*, 1324–1334.

Wang, S.N., Xu, T.Y., Wang, X., Guan, Y.F., Zhang, S.L., Wang, P., and Miao, C.Y. (2016). Neuroprotective efficacy of an aminopropyl carbazole derivative P7C3-A20 in ischemic stroke. CNS Neurosci. Ther. *22*, 782–788.

Zhang, L., Li, P., Hsu, T., Aguilar, H.R., Frantz, D.E., Schneider, J.W., Bachoo, R.M., and Hsieh, J. (2011). Small-molecule blocks malignant astrocyte proliferation and induces neuronal gene expression. Differentiation *81*, 233–242.

Zhang, Y., Li, W.L., Laurent, T., and Ding, S. (2012). Small molecules, big roles—the chemical manipulation of stem cell fate and somatic cell reprogramming. J. Cell Sci. *125*, 5609–5620.

Zhang, L., Yin, J.C., Yeh, H., Ma, N.X., Lee, G., Chen, X.A., Wang, Y., Lin, L., Chen, L., Jin, P., et al. (2015). Small molecules efficiently reprogram human astroglial cells into functional neurons. Cell Stem Cell *17*, 735–747.

Zhang, M.L., Lin, Y.H., Sun, Y.J., Zhu, S.Y., Zheng, J.S., Liu, K., Cao, N., Li, K., Huang, Y.D., and Ding, S. (2016). Pharmacological reprogramming of fibroblasts into neural stem cells by signaling-directed transcriptional activation. Cell Stem Cell *18*, 653–667.

Zhao, Y., Londono, P., Cao, Y., Sharpe, E.J., Proenza, C., O'Rourke, R., Jones, K.L., Jeong, M.Y., Walker, L.A., Buttrick, P.M., et al. (2015). High-efficiency reprogramming of fibroblasts into cardiomyocytes requires suppression of pro-fibrotic signalling. Nat. Commun. *6*, 8243.

Zhu, S., Li, W., Zhou, H., Wei, W., Ambasudhan, R., Lin, T., Kim, J., Zhang, K., and Ding, S. (2010). Reprogramming of human primary somatic cells by OCT4 and chemical compounds. Cell Stem Cell *7*, 651–655.